CELL STRUCTURE AND FUNCTION 32: 101–113 (2007)


# Implication of Amphiphysin 1 and Dynamin 2 in Tubulobulbar Complex Formation and Spermatid Release

**Norihiro Kusumi[1,2,†], Masami Watanabe[1,†], Hiroshi Yamada[2], Shun-Ai Li[2], Yuji Kashiwakura[3], Takashi Matsukawa[4], Atsushi Nagai[1], Yasutomo Nasu[1], Hiromi Kumon[1], and Kohji Takei[2*]**

*[1]Department of Urology, Graduate School of Medicine, Dentistry and Pharmaceutical Sciences, Okayama University, [2]Department of Neuroscience, Graduate School of Medicine, Dentistry and Pharmaceutical Sciences, Okayama University, [3]Center for Gene and Cell Therapy, Graduate School of Medicine, Dentistry and Pharmaceutical Sciences, Okayama University, 700-8558, Okayama, Japan, [4]Department of Anesthesia, University of Yamanashi, Faculty of Medicine, 400-8510, Yamanashi, Japan*

*ABSTRACT.* **Tubulobulbar complexes (TBCs) are composed of several tubular invaginations formed at the plasma membrane of testicular Sertoli cells. TBCs are transiently formed at the contact region with spermatids at spermatogenic stage VII in rat and mouse, and such TBC formation is prerequisite for spermatid release. Since the characteristic structure of TBCs suggests that the molecules implicated in endocytosis could be involved in TBC formation, we here investigated the localization and physiological roles of endocytic proteins, amphiphysin 1 and dynamin 2, at TBCs. We demonstrated by immunofluorescence that the endocytic proteins were concentrated at TBCs, where they colocalized with cytoskeletal proteins, such as actin and vinculin. Immunoelectron microscopy disclosed that both amphiphysin 1 and dynamin 2 were localized on TBC membrane. Next, we histologically examined the testis from amphiphysin 1 deficient {*Amph*$^{-/-}$} mice. Morphometric analysis revealed that the number of TBCs was significantly reduced in *Amph*$^{-/-}$. The ratio of stage VIII seminiferous tubules was increased, and the ratio of stage IX was conversely decreased in *Amph*$^{-/-}$. Moreover, unreleased spermatids in stage VIII seminiferous tubules were increased in *Amph*$^{-/-}$, indicating that spermatid release and the following transition from stage VIII to IX was prolonged in *Amph*$^{-/-}$ mice. These results suggest that amphiphysin 1 and dynamin 2 are involved in TBC formation and spermatid release at Sertoli cells.**

**Key words:** amphiphysin 1/dynamin 2/tubulobulbar complex/spermatogenesis/testis/endocytosis

## *Introduction*

In testis, Sertoli cells support germ cells at all spermatogenetic stages from spermatogonia to spermatid prior to the release into the lumen of the seminiferous tubules. Spermatogenic stages in rat seminiferous tubules are categorized into XIV stages, and the spermatid maturation is classified into 19 steps (Leblond and Clermont, 1952). At the interface to germ cells, Sertoli cells develop the unique adherent junctions named "ectoplasmic specialization" (ES) (Russell, 1977; 1979a). In rat Sertoli cells, the ES starts to appear when neighboring germ cells become step 8 round spermatids, and it disappears prior to the release of mature step 19 spermatids (Russell, 1977). Junctional structures termed tubulobulbar complexes (TBCs) are also formed between Sertoli cells near the basal surface of the seminiferous tubules, which functions as a blood-testis barrier (Russell, 1979a). The ES consists of a bundle of actin filaments sandwiched by Sertoli cell plasma membrane and the endoplasmic reticulum (Russell, 1977; 1979a).

TBCs, which are composed of several tubular invaginations at plasma membrane of Sertoli cells, are transiently formed at the contact region with spermatids right before the spermatid release (Russell and Clermont, 1976; Russell, 1979b; 1979c). These tubules have bulbar ends, and the plasma membrane of spermatids evaginates into the TBCs tubules (Russell, 1979b). TBCs are present in a variety of mammals including rat, mouse, hamster, rabbit, dog, monkey and human (Russell and Malone, 1980). In rat, TBCs

*To whom correspondence should be addressed: Kohji Takei, Department of Neuroscience, Graduate School of Medicine, Dentistry and Pharmaceutical Sciences, Okayama University, Okayama 700-8558, Japan.
Tel: +81–86–235–7120, Fax: +81–86–235–7126
E-mail: kohji@md.okayama-u.ac.jp
†Norihiro Kusumi and Masami Watanabe: These authors contributed equally to this study.

were observed at the luminal region of stage VII seminiferous tubules (Russell, 1979b), where they are enriched in cell cytoskeletal and adherent molecules such as actin, vinculin, cofilin, cortactin, nectin, and cadherin (Grove *et al*., 1990; Mulholland *et al*., 2001; Chapin *et al*., 2001; Guttman *et al*., 2004a; Lee and Cheng, 2004a; 2004b). As to the cell biological function of TBC, two possibilities have been suggested. One is that TBCs play a role in disassembly and/or removal of the ES structures (Guttman *et al*., 2004b). This is supported by observations in rat that when adherent ESs between Sertoli cells and spermatids start to disappear at stage VII, TBCs concomitantly appear in the area where the ES disappears (Russell and Clermont, 1976; Russell, 1979b; 1979c; Russell and Malone, 1980). Spermatids are released right after the removal of ES in stage VIII (Leblond and Clermont, 1952). The other possibility is that TBC functions as an endocytic device of Sertoli cells to uptake cytoplasm and acrosome of spermatids (Russell, 1979c; Tanii *et al*., 1999). Such TBC-mediated uptake decreases the cytoplasm of spermatid to 30% in volume, which shifts the spermatid to step 19, the completely matured germ cells (Russell, 1979c). TBCs are eventually separated from the plasma membrane of Sertoli cells, and transported to the lysosomes to be lysed (Russell, 1979b).

Sertoli cells have high endocytic activities (Clermont *et al*., 1987) and highly express endocytic proteins, such as amphiphysin and dynamin (Nakata *et al*., 1993; Watanabe *et al*., 2001; Kamitani *et al*., 2002; Iguchi *et al*., 2002), which are considered to participate in tubulization of plasma membrane (Takei *et al*., 1998; 1999; Ochoa *et al*., 2000). Amphiphysin 1 is highly present in Sertoli cells (Watanabe *et al*., 2001), whereas dynamin 2 is present in both Sertoli cells and germ cells (Kamitani *et al*., 2002; Iguchi *et al*., 2002). The function of amphiphysin 1 and dynamin 2 in Sertoli cells remains to be elucidated. However, from the functional analysis of these proteins in neurons, it is reasonable to assert that these proteins are involved in endocytosis. Amphiphysin 1 is also enriched in the synapse, where it cooperates with dynamin 1 in clathrin-mediated endocytosis (Takei *et al*., 1999). The SH3 domain of amphiphysin 1 interacts directly with the proline-rich domain of dynamin 1, and the binding of amphiphysin 1 to dynamin 1 results in the stimulation of dynamin GTPase activity (Takei *et al*., 1999; Yoshida *et al*., 2004). The N-terminal BAR (BIN/amphiphysin/Rvs) domain of amphiphysin 1 forms a crescent-shaped dimer that binds preferentially to a curved lipid membrane, and therefore it is proposed to function in sensing membrane curvature (Peter *et al*., 2004).

Amphiphysin 1 is involved not only in clathrin-mediated endocytosis (Takei *et al*., 1998; 1999), but also in regulation of actin cytoskeleton (Mundigl *et al*., 1998; Balguerie *et al*., 1999; Friesen *et al*., 2003). Rvs 167 protein, an amphiphysin homologue in yeast, localized at actin patch, and disruption of the gene resulted in defect in actin cytoskeleton (Balguerie *et al*., 1999; Friesen *et al*., 2003). In neurons, a pool of amphiphysin 1 was colocalized with actin patches at the edge of growth cone (Mundigl *et al*., 1998). Dynamin 2 is also implicated in actin dynamics (Witke *et al*., 1998; Lee and DeCammili, 2002; Orth and McNiven, 2003; Schafer *et al*., 2004), and a key molecule that links endocytosis and actin cytoskeleton is cortactin, which binds to both dynamin 2 and F-actin (McNiven *et al*., 2000; Cao *et al*., 2003).

In this study, we examined the localization of amphiphysin 1 and dynamin 2 in rat testis by immunofluorescence and electron microscopy. Using amphiphysin 1 deficient mice, we also investigated the possible function of amphiphysin 1 on TBC during spermatogenesis.

## *Materials and Methods*

### *Animals*

Male Wistar rats (8–9 week old, weight 200–250 g) were purchased from Shimizu Laboratory Supplies Co. (Kyoto, Japan). Amphiphysin 1 deficient mice (*Amph*$^{-/-}$), which were generated by gene targeting in embryonic stem cells as described previously (Di Paolo *et al*., 2002), were provided by Professor Pietro De Camilli (Yale University). Twenty-week-old C57BL/6 (wild-type) or *Amph*$^{-/-}$ mice were used for experiments. All animals were maintained under clean conditions with free access to food and water. They were allowed to adapt to their environment for more than 1 week before initiating the experiments.

### *Antibodies and reagents*

Mouse monoclonal anti-amphiphysin 1 antibody and rabbit polyclonal anti-amphiphysin 1 antibody were gifts from Professor Pietro De Camilli (Takei *et al*., 1998). Goat polyclonal antibody against dynamin 2 was obtained from Santa Cruz Biotechnology (Santa Cruz, CA). Rabbit polyclonal antibody against dynamin 3 was obtained from ABR (Golden, CO). Mouse monoclonal anti-vinculin antibody was obtained from Sigma (St. Louis, MO). Alexa 488-conjugated goat anti-mouse, Alexa 546-conjugated donkey anti-goat IgG and Alexa 488-conjugated phalloidin were from Molecular Probes (Eugene, OR). Ten nm colloidal gold particles conjugated with goat anti-rabbit IgG were from BB International (Llanishen, UK). 4',6-diamidino-2-phenylindol-dihydrochloride (DAPI) was from Kirkegaard & Perry Laboratories, Inc. (Gaithersburg, MD).

### *Western blotting*

Testis and brain from 21-day-old Wistar rat were used for the tissue lysate. Sertoli cells and germ cells of the rat testes were sampled separately as described elsewhere (Kamitani *et al*., 2002). Western blot analysis was performed using the lysates as described (Kamitani *et al*., 2002). Briefly, 30 μg of total proteins/lane was electrophoresed on 6% SDS-PAGE. The blotted membranes were

blocked with 5% skim milk, 0.5% bovine serum albumin (BSA) in 25 mM Trizma base, 1 mM EDTA, and 140 mM NaCl (TEN). The membrane was incubated with primary antibodies diluted at 1:1000 in TEN containing 0.05% Tween 20 for 2 hr at room temperature, and then with HRP-conjugated secondary antibodies diluted at 1:5000 for 1 hr. Immunoreactive bands were visualized by enhanced chemiluminescence (ECL; Amersham, Chicago, IL).

### *Light microscopy*

Mouse testis was immersion-fixed with Bouin's solution for more than 5 hr, and embedded in paraffin. Ten μm-sections were cut and stained with hematoxylin-eosin. For staging of each seminiferous tubule, periodic acid-Schiff (PAS) and hematoxylin staining was performed as described (Oakberg *et al*., 1956a). For immunohistochemistry, rats were deeply anesthetized by intraperitoneal injection with sodium pentobarbital (30 mg/kg) and the testis was fixed by transcardiac perfusion with 4% paraformaldehyde in 100 mM phosphate buffer, pH 7.4 for 20 min at 4°C. The testis was sliced into 5 mm thick slabs, and postfixed in the same fixative for 12 hr, and then cryoprotected with 12%, 16%, 18% sucrose. Five μm thick sections were cut using a cryostat. Sections were incubated with primary antibodies (anti-amphiphysin 1 monoclonal antibody and anti-dynamin 2 antibody at dilution 1:100, and anti-vinculin antibody at a dilution 1:200) for 6 hr at room temperature and then with fluorescence-conjugated secondary antibodies for 1 hr. Alexa 488-conjugated phalloidin was used for actin staining at a dilution of 1:40. The sections were then counterstained with DAPI to visualize the nucleus.

### *Electron microscopy*

Testis was fixed by transcardial perfusion with 3% glutaraldehyde in 100 mM phosphate buffer for 20 min at 4°C. The testis was dissected and cut into 3 mm cubes, and fixed in the same fixative for 6 hr and further fixed in 1% $OsO_4$ for 3 hr. Specimens were embedded in Epon 812. One μm sections were cut to identify stage VII seminiferous tubules before sectioning ultrathin sections. For immunoelectron microscopy, testis was fixed with 4% paraformaldehyde and 0.1% glutaraldehyde in 100 mM phosphate buffer (pH 7.4) at 4°C. Fixed samples were dehydrated with 50%, 70%, 90%, 99% ethanol, and then embedded in LR White (London Resin Company Ltd., Basingstoke, UK). Ultrathin sections on nickel grids were incubated with 6 M urea in 50 mM glycine-HCl buffer (pH 3.5) for 5 min. Grids were blocked with 10% fetal bovine serum in 100 mM phosphate buffer, incubated with primary antibodies (anti-amphiphysin 1 polyclonal antibody or anti-dynamin 2 antibody at a dilution 1:20) overnight at room temperature, and then with immunogold particle-conjugated secondary antibodies for 1 hr. Ultrathin sections were observed with an H-7100S transmission electron microscope (Hitachi, Tokyo, Japan).

### *Morphometric analysis*

Spermatogenic stages in rat seminiferous tubules are categorized into XIV stages, and spermatid maturation is classified into 19 steps (Leblond and Clermont, 1952). Those in mouse are categorized into XII stages and 16 steps as described (Oakberg, 1956a; Abe *et al*., 1991). For quantitative analysis of spermatogenic stages in mouse, a total of 1000 seminiferous tubules from 5 mice of wild-type or *Amph*$^{-/-}$ testis were randomly examined under light microscope. The number of tubules in each spermatogenic stages was counted, and the percentage of each stage in the total seminiferous tubules was calculated as previously described (Oakberg, 1956b). The percentage value is proportional to the total length of each stage in the tubules. The number of unreleased spermatids per length in stage VIII seminiferous tubule was calculated as follows. Randomly selected 100 cross-sections of stage VIII tubules from 5 mice were photographed in each genotype, and the number of unreleased spermatids was counted. The longer and shorter diameters of internal seminiferous circle were measured to determine the length of the circle. The length was calculated using the formula, $\pi\times\sqrt{(2\times(L^2+S^2))}$ (where $L$ and $S$ are longer and shorter radii, respectively). From these counts and measurements, the number of unreleased spermatids per length was assessed. To analyze the frequency of appearance of TBCs in wild-type and *Amph*$^{-/-}$ mice, the portions of Sertoli cells surrounded by step 16 spermatids at stage VII were randomly photographed by electron microscopy. More than 100 areas from 3 mice of each genotype were subjected to morphometry. To demonstrate by immunoelectron microscopy that amphiphysin 1 and dynamin 2 are concentrated with close proximity at the plasma membrane invagination, the number of immunogold particles separated by a certain distance (either within 100 nm or 100–200 nm) from TBC was counted in the sections. To avoid inadvertent bias, all morphometric analyses were carried out by blind ssessors. All data are presented as the mean±SD. Mann-Whitney U-test was used for statistical analysis of the morphometric difference. Differences were considered significant if $p<0.05$.

## *Results*

### *Spermatogenic stage-specific localization of amphiphysin 1 and dynamin 2 in rat testis*

We first confirmed the expression of amphiphysin 1 and dynamin 2 in rat testis by western blot analysis. The result revealed that amphiphysin 1 was expressed highly in Sertoli cells (Fig. 1a) and dynamin 2 was present in both Sertoli cells and germ cells (data not shown), showing the consistency with previous reports (Watanabe *et al*., 2001; Kamitani *et al*., 2002; Iguchi *et al*., 2002). Next, immunohistochemistry was performed to determine their localizations in rat seminiferous tubules at different spermatogenetic stages. Immunoreactivities for amphiphysin 1 were present in Sertoli cells in all stages of seminiferous tubules (Fig. 1b, Fig. 2a, e, i, and data not shown). It was noted that amphiphysin 1 was highly accumulated at luminal surface in a subset of seminiferous tubules (Fig. 1b). In such tubules, dynamin 2 was also concentrated at the luminal region,

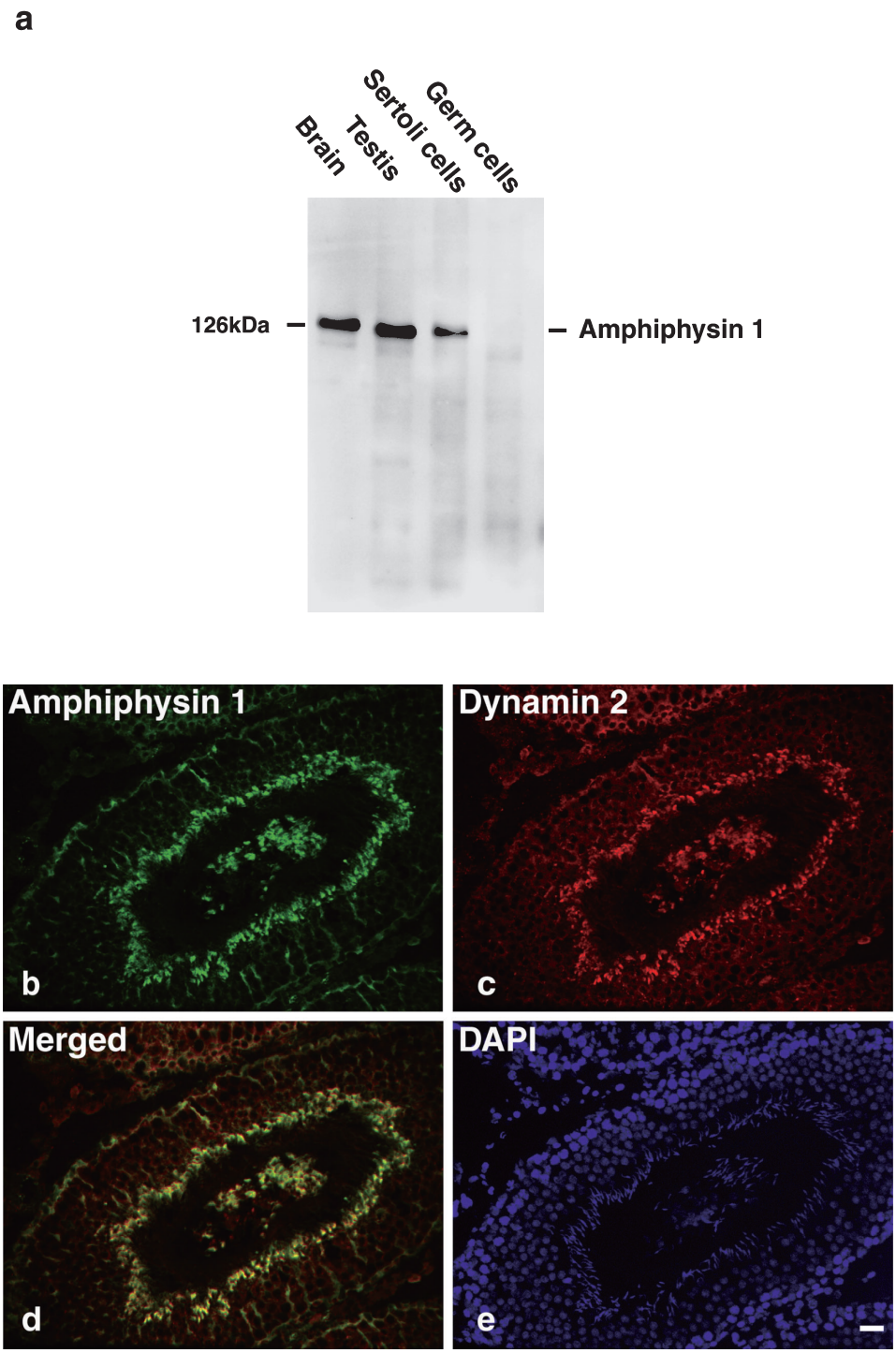


**Fig. 1.** (a) Expression of amphiphysin 1 in rat testis was revealed by Western blot analysis. Note that amphiphysin 1 is highly expressed in Sertoli cells. (b–e) Colocalization of amphiphysin 1 and dynamin 2 at luminal surface of rat spermatogenic stage VII seminiferous tubule was demonstrated by double immunofluorescence. Amphiphysin 1 and dynamin 2 were present at the innermost layer of seminiferous tubules (b, c). Colocalization of these proteins was shown (d). Elongated spermatids were arranged at the innermost layer (e). Calibration bar represents 20 μm in (b–e).

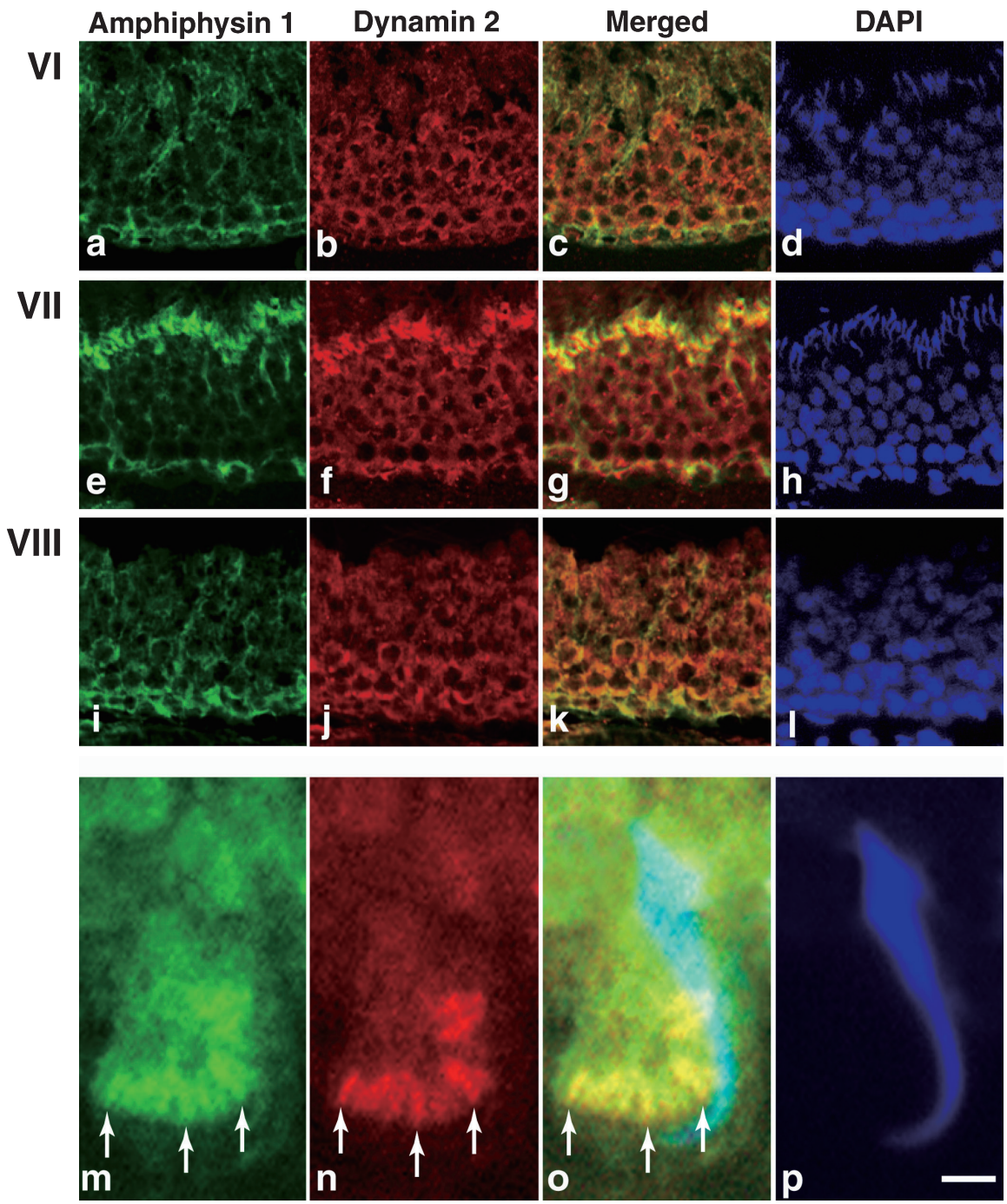


**Fig. 2.** Stage specific expression of amphiphysin 1 and dynamin 2 in rat (a–l). Amphiphysin 1 (e) and dynamin 2 (f) were highly expressed at the innermost layer of seminiferous tubules at stage VII, where spermatids at step 19 were arranged (h). Note the colocalization of amphiphysin 1 and dynamin 2 at region (g). Colocalization was specific to stage VII, and was not observed at stage VI (a–d) and stage VIII (i–l). At high magnification of the innermost layer of rat seminiferous tubule in stage VII (m–p), amphiphysin 1 (m) and dynamin 2 (n) were concentrated at the Sertoli cell cytoplasm adjacent to the curvature of the innermost spermatids (p). Immunoreactivity for amphiphysin 1 and dynamin 2 was expressed as periodically arranged rods (arrows in m–o). The periodicity was less evident for amphiphysin 1 (m) than for dynamin 2 (n). (c), (g), (k) are merged images for (a) and (b), (e) and (f), (i) and (j), respectively. Merged image for (m), (n) and (p) is shown in (o). Calibration bar represents 20 μm in (a–l) and 2.5 μm in (m–p).

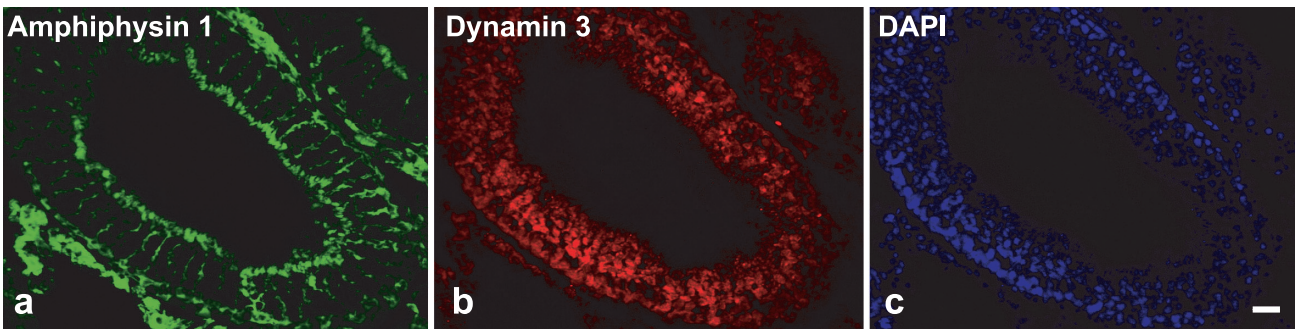


**Supplementary fig. 1.** Localization of amphiphysin 1 (a) and dynamin 3 (b) in rat spermatogenic stage VII seminiferous tubule. The section was labeled by double immunofluorescence. Note the absence of dynamin 3 at the luminal surface. Bar: 20 μm.

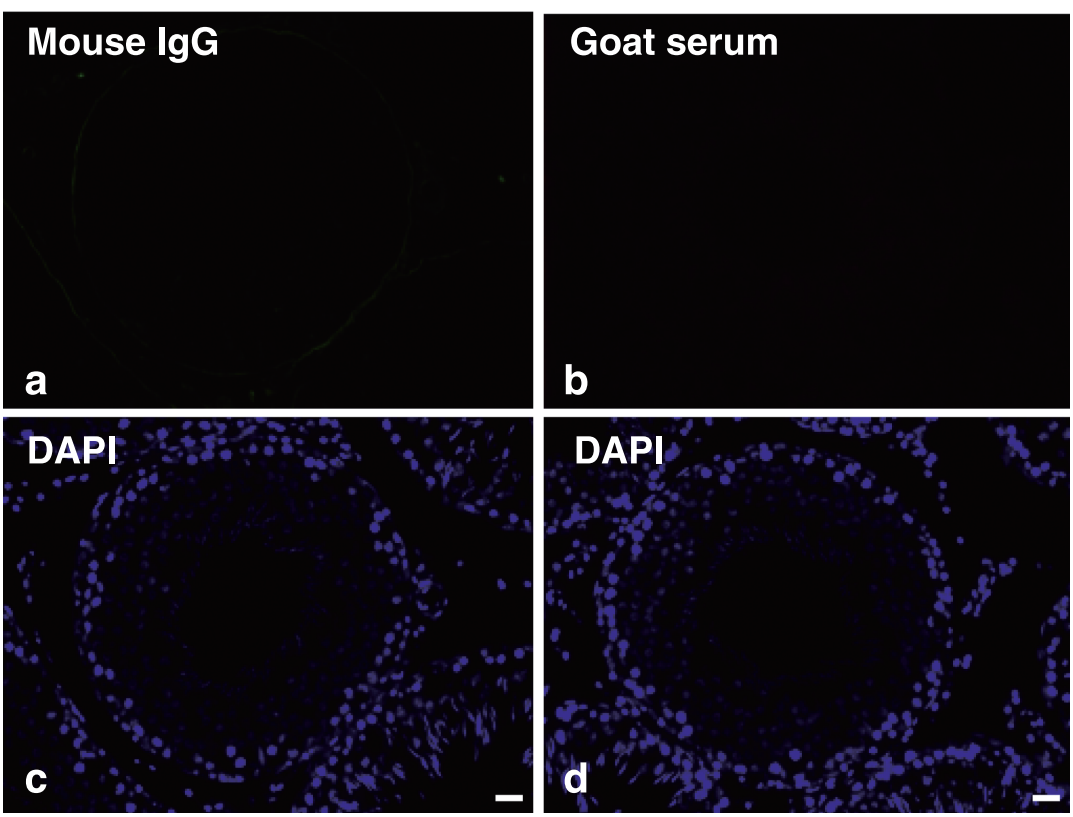


**Supplementary fig. 2.** Control immunofluorescence experiments showing that virtually no signal is detected with mouse IgG (a) or goat serum (b) on seminiferous tubules. The sections were counterstained with DAPI (c and d). Bar; 20 μm.

where it colocalized with amphiphysin 1 (Fig. 1b–d). By DAPI staining, it was revealed that the seminiferous tubules expressing amphiphysin 1 and dynamin 2 at the luminal surface contained elongated spermatids arranged along the inner surface (Fig. 1e). From the typical arrangement of spermatids, the tubules were identified as stage VII (Fig. 2e–h). Concentration of dynamin 2 and amphiphysin 1at luminal surface was not observed in the other stages including stage VI (Fig. 2a–d), where spermatids are present but not well aligned at the luminal surface, or stage VIII (Fig. 2i–l), where the mature spermatids have been released and are no longer present in the lumen. At high magnification, amphiphysin 1 and dynamin 2 at stage VII were present at apical regions of Sertoli cells facing to the concave side of sickle-shaped spermatid heads (Fig. 2m–p). In these regions, the immunoreactivities for dynamin 2 were recognized as periodically arranged bars (arrows in Fig. 2n). The periodicity of immunoreactivity was also observed, although less

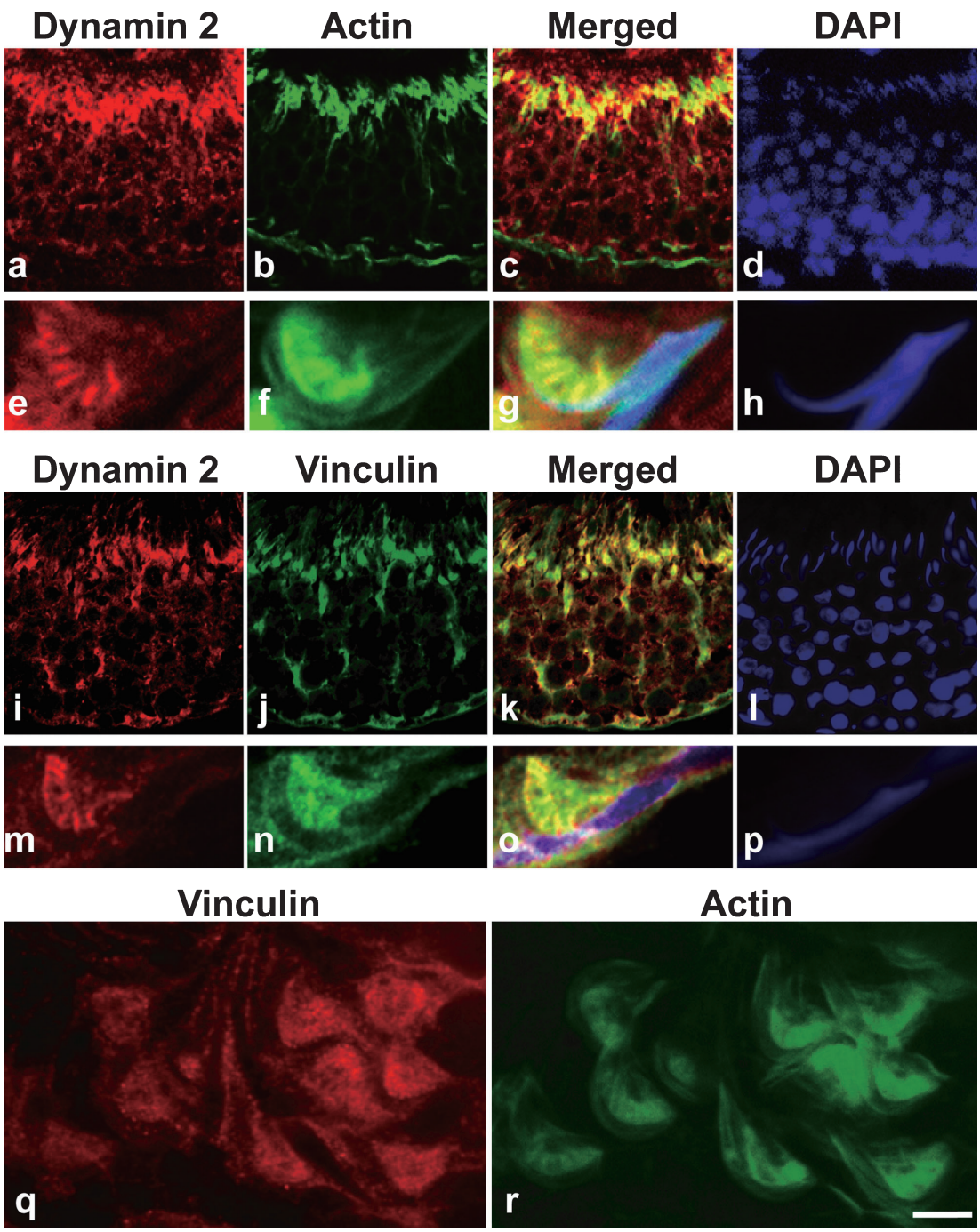


**Fig. 3.** Colocalization of dynamin 2 with cell cytoskeletal molecules in rat (a–p). Dynamin 2 and actin were highly expressed at the luminal surface of stage VII at low magnification (a–d). Dynamin 2 was colocalized with actin at TBCs at high magnification (e–h). Dynamin 2 and vinculin were highly expressed at the luminal surface of stage VII at low magnification (i–l). Dynamin 2 was colocalized with vinculin at TBCs at high magnification (m–p). Vinculin and actin were present at inside of curved rat spermatids (q, r). Calibration bar represents 22 μm in (a–d) and (i–l), 3 μm in (e–h) and (m–p), and 5 μm in (q, r).

clearly, for amphiphysin 1 (arrows in Fig. 2m). These two proteins were well colocalized within the region (arrows in Fig. 2o). Dynamin 3, another isoform highly expressed in Sertoli cells and germ cells (Kamitani *et al*., 2002), was not concentrated at TBC region (Supplementary fig. 1). Nonimmune IgG or serum controls were analyzed for the antibodies and there were no specific signals (Supplementary fig. 2).

### *Amphiphysin 1 and dynamin 2 colocalize at TBC structures*

Given that amphiphysin 1 and dynamin 2 are endocytic proteins that have strong membrane tubulating activities (Takei *et al*., 1998; 1999; Ochoa *et al*., 2000), immunolocalization of these proteins at the luminal surface of stage VII was likely to represent the presence of the proteins at TBCs. Therefore, double immunofluorescence was performed using the constitutional and marker proteins for TBC, actin and vinculin (Grove *et al*., 1990; Mulholland *et al*., 2001; Chapin *et al*., 2001; Guttman *et al*., 2004a; Lee and Cheng, 2004a; 2004b). As expected, actin and vinculin were colocalized with dynamin 2 at the apical regions of Sertoli cells in stage VII (Fig. 3a–d and 3i–l). Like amphiphysin 1 and dynamin 2, actin and vinculin were absent on the luminal surface of seminiferous tubules at the other stages (data not shown). High magnification of stage VII revealed strong immunoreactivity of actin and vinculin at the region where periodical immunoreactivity of dynamin 2 was present (Fig. 3e–h and 3m–r). Taken together, this strongly suggested that amphiphysin 1 and dynamin 2 are present at TBC structures.

Next, we observed rat and mouse TBC structures by electron microscopy. TBCs were present in both rat (Fig. 4a, b) and mouse (Fig. 4c–e). TBCs were present where actin bundles of ES had disappeared (Fig. 4e), consistent with previous studies (Russell and Clermont, 1976; Russell, 1979b; 1979c; Russell and Malone; 1980). To investigate localization of amphiphysin 1 and dynamin 2 at TBCs in detail, immunoelectron microscopy was performed. Expectedly, both amphiphysin 1 and dynamin 2 were present at the area adjacent to the membrane invagination of a Sertoli cell (Fig. 5a, c). Morphometric analysis confirmed that these proteins were concentrated in proximity to the plasma membrane invagination of TBC (Fig. 5b, d). No specific signals were observed with nonimmune serum (Supplementary fig. 3).

### *Deletion of amphiphysin 1 reduces the number of TBCs and affects spermatogenic stages in mouse*

Electron microscopy also revealed that the TBC structures were often present where Sertoli cells surround step 16 spermatids (Fig. 6a). By Western blotting, a similar level of dynamin 2 expression was observed in wild-type and

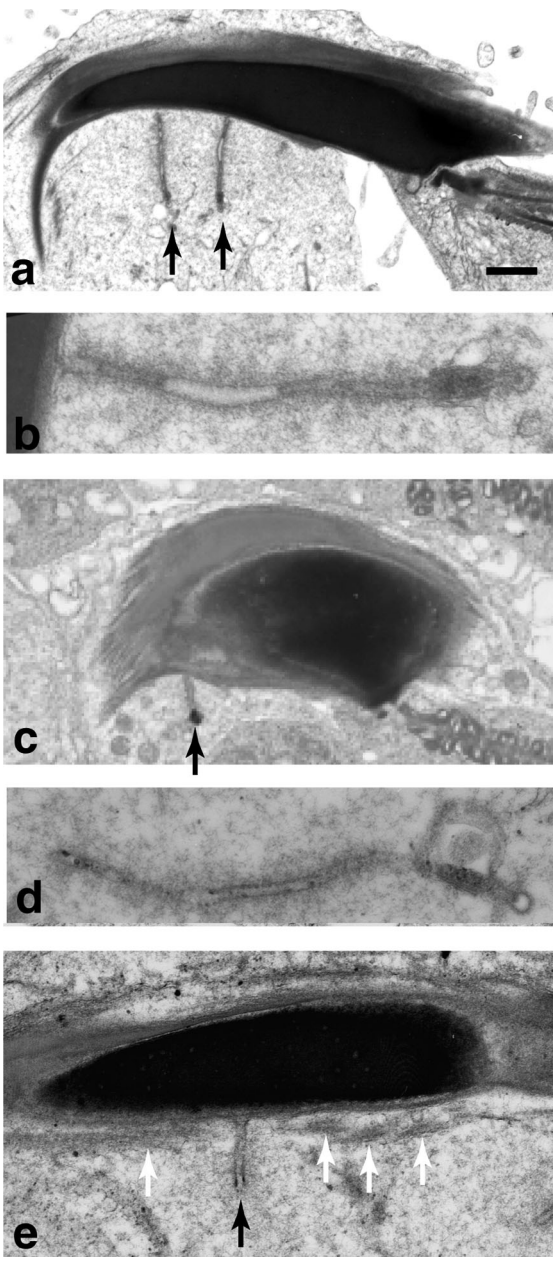


**Fig. 4.** Ultrastructure of TBC in rat (a, b) and wild-type mouse (c, d, e) by electron microscopy. Sections in (a–d) were cut along the long axis of the elongated spermatids. Tubular membrane invaginations of TBC (black arrow) of approximately 50–100 nm in diameter were formed in the Sertoli cells adjacent to the inner curvature of the elongated spermatids (a, c, e). The tubular structure was connected to the plasma membrane of the Sertoli cell (b, e). Tubular membrane invaginations of TBC were generated at the region where actin bundles of ES (white arrow) were absent (e). Calibration bar represents 1 μm in (a, c), 200 nm in (b, d) and 400 nm in (e).

*Amph*$^{-/-}$ testis (Supplementary fig. 4). Since the transient formation of TBCs coincided with the presence of amphiphysin 1 and dynamin 2 in the region, we next examined

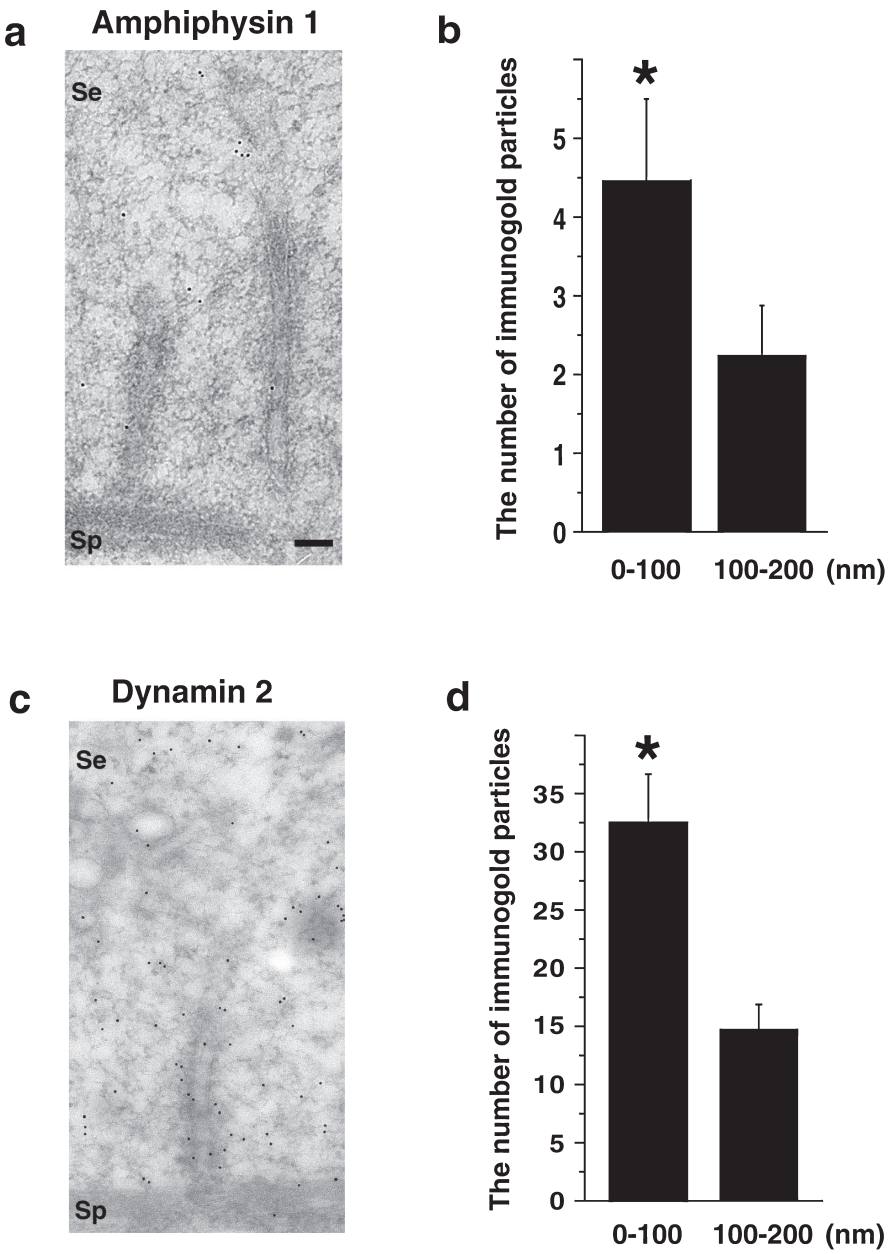


**Fig. 5.** Immunoelectron microscopy for amphiphysin 1 and dynamin 2 at rat TBC structure (a–d). Immunogold particles labeling amphiphysin 1 (a) and dynamin 2 (c) were located on or near the plasma membrane of TBC. To confirm that amphiphysin 1 and dynamin 2 are concentrated in close proximity at the plasma membrane invagination, the number of immunogold particles separated a distance (within 100 nm or 100–200 nm) from TBC was counted in the sections. In both proteins labeling the TBC, the number of immunogold particles located within 100 nm was significantly high compared to that in 100–200 nm area. (b) amphiphysin 1: *: $p<0.01$, number of observed TBCs=34. (d) dynamin 2: *: $p<0.01$, number of observed TBCs=14. Calibration bar represents 160 nm in (a, c). Se: Sertoli cell. Sp: spermatid.

whether the appearance of the TBC structures is affected by amphiphysin 1. For this purpose, we counted the number of membrane invaginations of TBC present in wild-type or *Amph*$^{-/-}$ Sertoli cells (Fig. 6a, b). The number of membrane tubules was apparently reduced in *Amph*$^{-/-}$ testis compared to the wild-type (Fig. 6c: 4.51±0.24 in wild-type and 1.82±0.21 in *Amph*$^{-/-}$). Given that TBC formation has a close link with the removal of the ES structures and with spermatid release (Guttman *et al*., 2004b; Mruk and Cheng, 2004), the reduction of TBC tubules in *Amph*$^{-/-}$ testis prompted us to investigate whether the spermatogenic cycle and the spermatid release were affected in *Amph*$^{-/-}$ testis. The ratio of

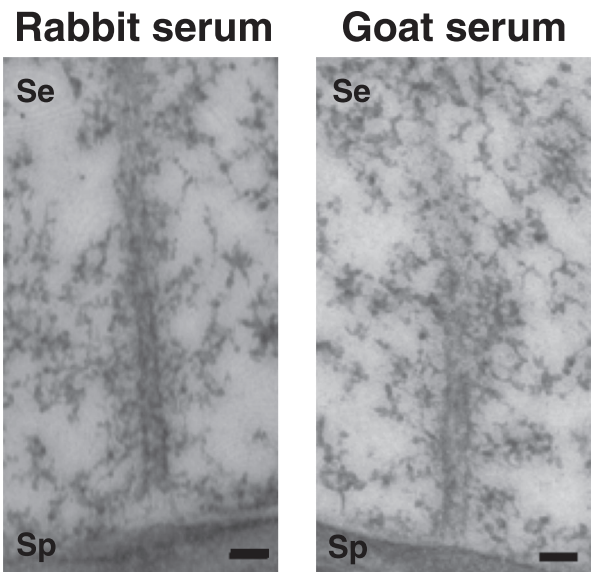


**Supplementary fig. 3.** Control immunogold experiments showing that no signal is detected with rabbit serum (left) or goat serum (right) on TBC. Bar; 160 nm.

stage VIII was significantly increased in *Amph*$^{-/-}$ mice compared to the wild-type mice (Fig. 7a). The compensatory decrease of stage IX, a stage immediately after the spermatid release, was also apparent in *Amph*$^{-/-}$ testis. There was no significant difference in the other stages. We defined seminiferous tubule stage with the latest spermatids as stage VIII. Therefore, spermatids were absent in stage IX and X. The effect of the delayed release in the KO is reflected as the increase of stage VIII (Fig. 7a). The number of unreleased spermatids at stage VIII was consistently increased to approximately twofold in *Amph*$^{-/-}$ testis (Fig. 7b).

## *Discussion*

The present study demonstrated that amphiphysin 1 and dynamin 2 are concentrated at the luminal surface of seminiferous tubules at stage VII. A combination of immunofluorescence and immunoelectron microscopy revealed that these proteins concentrate on the plasma membrane of TBC at stage VII. This is the first demonstration that these endocytic proteins are enriched at the TBC. The TBC consists of a variety of molecules implicated in cytoskeleton and cell attachment, such as actin, vinculin, cofilin, cortactin, nectin, and cadherin (Grove *et al*., 1990; Mulholland *et al*., 2001; Chapin *et al*., 2001; Guttman *et al*., 2004a; Lee and Cheng, 2004a; 2004b). Amphiphysin 1 and dynamin 2 colocalized with actin and vinculin (in this study) and cortactin (data not shown) around TBC, which implicates these endocytic proteins in the TBC function via cytoskeletal modulation.

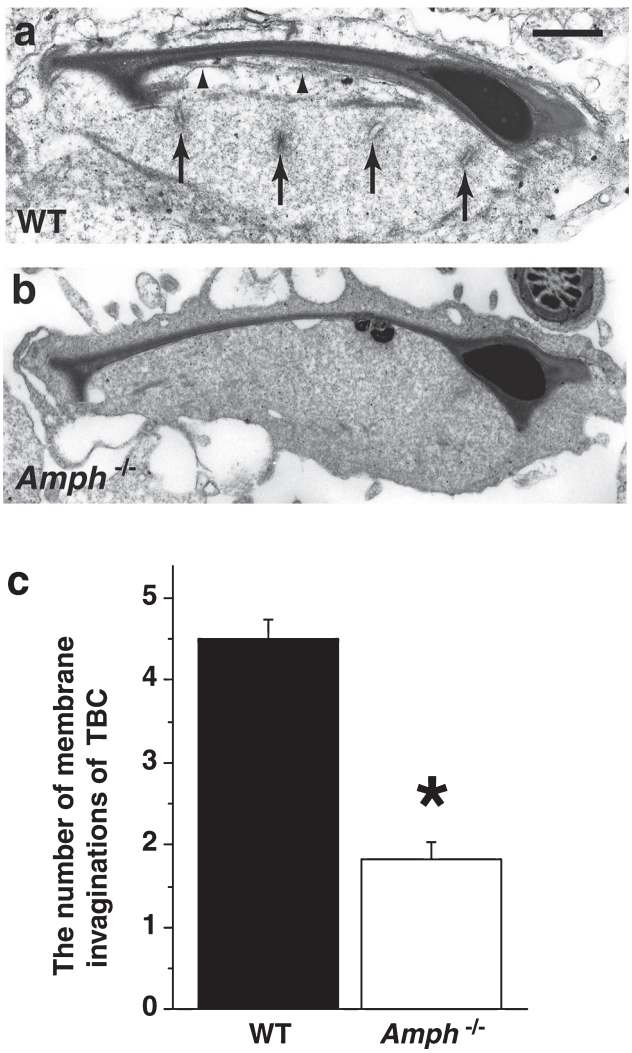


**Fig. 6.** Frequency of TBC structures at the apical cytoplasm of a Sertoli cell was compared between wild-type (WT) and *Amph*$^{-/-}$ mice (a–c). TBC is shown using an arrow. ES structures are shown using arrowheads. In the morphometric analysis of TBCs in number (c), the frequency of TBCs in *Amph*$^{-/-}$ mice was approximately half of that in WT mice (*: $p<0.0001$, number of observations in each genotype=102). Calibration bar in (a) represents 1 μm in (a, b).

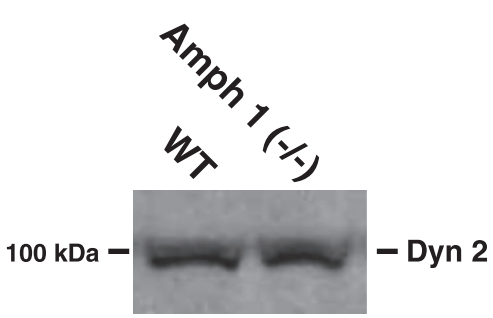


**Supplementary fig. 4.** Western blot analysis showing presence of similar amounts of dynamin 2 in WT or amphiphysin 1 (–/–) mouse testis.

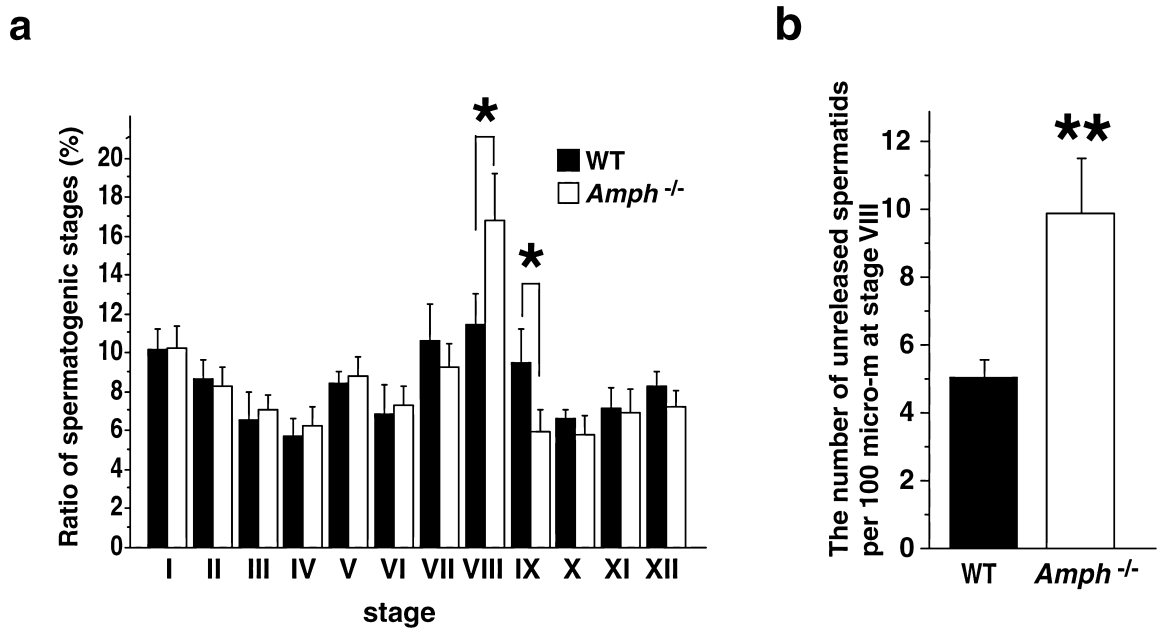


**Fig. 7.** Quantitative analysis of spermatogenic stages in WT and *Amph*$^{-/-}$ mice (a). The ratio of stage VIII and stage IX in *Amph*$^{-/-}$ mice was significantly higher and lower than that in WT mice, respectively (*: $p<0.05$, no. of mice=5). Quantitative analysis of unreleased spermatids at stage VIII in WT and *Amph*$^{-/-}$ mice (b). The number of unreleased spermatids in *Amph*$^{-/-}$ mice was increased to about twofold compared to that in WT mice (**: $p<0.01$, number of mice=5).

Morphometrical analysis revealed the reduction of TBC in number in *Amph*$^{-/-}$ testis. This result could be attributed either to increased fission activity of TBC, and/or reduced generation of TBC in *Amph*$^{-/-}$ testis. Since suppression of amphiphysin 1 expression in cultured Sertoli cells had no effect on transferrin uptake (data not shown), amphiphysin 1 at the apical region may function in the TBC formation rather than fission. As to how amphiphysin 1 contributes to TBC formation, there are two possibilities. One is that the amphiphysin family proteins with the N-terminal BAR domain, which sense membrane curvature and could tubulate the membrane (Peter *et al*., 2004), participate in TBC formation. The amphiphysin isoform, amphiphysin 2 (also called BIN1), is localized at the T-tubule, which is a TBC-like membrane invagination in skeletal muscle, and plays a role in T-tubule formation (Butler *et al*., 1997; Lee *et al*., 2002). A second possibility is that the interaction between amphiphysin 1 and/or dynamin 2 and other proteins acts on the actin depolymerization required for TBC formation. Peripheral actin in Sertoli cells transiently forms clear actin bundles sandwiched between the plasma membrane and the endoplasmic reticulum. The structure of the cell-cell actin-based adherent junction (ES) is dissolved concomitant with TBC formation at the interface between Sertoli cells and spermatids. Application of cytochalasin D, an inhibitor of F-actin formation, results in the destruction of ES and TBC formation in rat testis, suggesting that actin depolymerization is required for TBC formation (Russell *et al*., 1988; Mruk and Cheng, 2004). Actin filament bundles in ES are either depolymerized or fragmented and the formation of TBCs is then initiated in part by the recruitment of actin network-forming proteins to the site.

The involvement of endocytic proteins in actin cytoskeleton has been occasionally reported. Rvs 167 protein, the yeast amphiphysin homologue, was colocalized with actin patches, and the mutation of the homologue led to abnormal actin cytomatrix (Balguerie *et al*., 1999). Phosphorylation of Rvs 167 protein regulated actin cytoskeleton in yeast (Friesen *et al*., 2003). By the analysis of cultured hippocampal neurons, amphiphysin 1 was shown to be colocalized with actin in the apex of dendritic and axonal growth cones (Mundigl *et al*., 1998). Amphiphysin 2 has also been shown to be concentrated at the actin layer in axons, the nodes of Ranvier, and muscle (Butler *et al*., 1997).

As for dynamin, dynamin 2 binds actin-binding proteins, such as cortactin (McNiven *et al*., 2000; Cao *et al*., 2003) and profilin (Witke *et al*., 1998) via its proline-rich domain, in an interaction that regulates cell shape (McNiven *et al*., 2000). Interestingly, dynamin 2 seems to be involved in the formation of the podosome, which is a TBC-like tubular membrane invagination observed in osteoclasts, fibroblasts, and macrophages (Ochoa *et al*., 2000). Both the podosome and the TBC of this study are enriched in dynamin 2 and actin filaments (Ochoa *et al*., 2000), suggesting that these proteins may play a role in the dynamics of tubular structure formation by modulating the cell cytoskeleton. Sertoli cells

express dynamin 3 in addition to dynamin 2. However, it is unlikely that dynamin 3 is implicated in the formation of TBC, since the isoform is not concentrated at TBC region in stage VII (Supplementary fig. 1). In contrast, the localization of dynamin 3 at TBC was recently reported (Vaid *et al*., 2007). The discrepancy may be caused by the difference of dynamin 3 antibodies used in the studies. Future studies are needed on the general function of dynamin 3 in testis.

This study revealed that the ratio of stage VIII seminiferous tubules in *Amph*$^{-/-}$ testis was significantly increased compared to that of control mice. Conversely, the ratio of stage IX in *Amph*$^{-/-}$ testis was decreased. The unreleased spermatids were increased in stage VIII in *Amph*$^{-/-}$ testis, indicating that the shift from stage VIII to IX by completing the spermatid release is prolonged in *Amph*$^{-/-}$ mice. However, it remains to be elucidated why an increase of unreleased spermatids was observed in the mice. Taken together with the current evidence that the number of TBCs was decreased in *Amph*$^{-/-}$ mice, there are two conceivable explanations to the phenomenon. First, it is possible that the complete resolution and/or removal of the adherent ES structure is being prolonged because of the decline in TBC number and function. In this case, it would seem that spermatid release is being directly inhibited by the delay of adherent ES absorption in Sertoli cells. Second, we conjectured that the cytoplasmic material from spermatids were not being efficiently endocytosed by the Sertoli cells due to the reduction in the number of TBC. The insufficient final formation of the spermatids by Sertoli cells could thus trigger the delay of spermatid maturation and the disruption of spermatid release.

In conclusion, we found that amphiphysin 1 and dynamin 2 were colocalized at TBCs, thus implicating them in the TBC formation and spermatid release that is the final step of spermatogenesis. To our knowledge, this is the first study to demonstrate the influence of the absence of amphiphysin 1 on spermatogenesis. Although further studies are required as to semen findings and reproducibility in *Amph*$^{-/-}$ mice, it is very likely that these proteins play an important role in endocytic systems and germ cell-supportive functions of Sertoli cells in order to promote spermatogenesis.

*Acknowledgements.* We wish to thank Professor Pietro De Camilli (Yale University) for providing the amphiphysin 1 deficient mice, and Masumi Furutani (Okayama University) for technical support with electron microscopy. This work was supported in part by the Central Laboratory Center of Okayama University, and by a Grant-in-aid from the Ministry of Education, Science, Sports, and Culture of Japan (to K. Takei and H. Kumon).

***References***

Abe, K., Shen, L.S., and Takano, H. 1991. The cycle of the seminiferous epithelium and stages in spermatogenesis in dd-mice. *Hokkaido Igaku Zasshi*, **66**: 286–299.

Balguerie, A., Sivadon, P., Bonneu, M., and Aigle, M. 1999. Rvs167p, the budding yeast homolog of amphiphysin, colocalizes with actin patches. *J. Cell Sci.*, **112**: 2529–2537.

Butler, M.H., David, C., Ochoa, G.C., Freyberg, Z., Daniell, L., Grabs, D., Cremona, O., and De Camilli P. 1997. Amphiphysin II (SH3P9; BIN1), a member of the amphiphysin/Rvs family, is concentrated in the cortical cytomatrix of axon initial segments and nodes of Ranvier in brain and around T tubules in skeletal muscle. *J. Cell Biol.*, **137**: 1355–1367.

Cao, H., Orth, J.D., Chen, J., Weller, S.G., Heuser, J.E., and McNiven, M.A. 2003. Cortactin is a component of clathrin-coated pits and participates in receptor-mediated endocytosis. *Mol. Cell Biol.*, **23**: 2162–2170.

Chapin, R.E., Wine, R.N., Harris, M.W., Borchers, C.H., and Haseman, J.K. 2001. Structure and control of a cell-cell adhesion complex associated with spermiation in rat seminiferous epithelium. *J. Androl.*, **22**: 1030–1052.

Clermont, Y., Morales, C., and Hermo, L. 1987. Endocytic activities of Sertoli cells in the rat. *Ann. N Y Acad. Sci.*, **513**: 1–15.

Di Paolo, G., Sankaranarayanan, S., Wenk, M.R., Daniell, L., Perucco, E., Caldarone, B.J., Flavell, R., Picciotto, M.R., Ryan, T.A., Cremona, O., and De Camilli, P. 2002. Decreased synaptic vesicle recycling efficiency and cognitive deficits in amphiphysin 1 knockout mice. *Neuron*, **33**: 789–804.

Friesen, H., Murphy, K., Breitkreutz, A., Tyers, M., and Andrews, B. 2003. Regulation of the yeast amphiphysin homologue Rvs167p by phosphorylation. *Mol. Biol. Cell*, **14**: 3027–3040.

Grove, B.D., Pfeiffer, D.C., Allen, S., and Vogl, A.W. 1990. Immunofluorescence localization of vinculin in ectoplasmic ("junctional") specializations of rat Sertoli cells. *Am. J. Anat.*, **188**: 44–56.

Guttman, J.A., Obinata, T., Shima, J., Griswold, M., and Vogl, A.W. 2004a. Non-muscle cofilin is a component of tubulobulbar complexes in the testis. *Biol. Reprod*., **70**: 805–812.

Guttman, J.A., Takai, Y., and Vogl, A.W. 2004b. Evidence that tubulobulbar complexes in the seminiferous epithelium are involved with internalization of adhesion junctions. *Biol. Reprod*., **71**: 548–559.

Iguchi, H., Watanabe, M., Kamitani, A., Nagai, A., Hosoya, O., Tsutsui, K., and Kumon, H. 2002. Localization of dynamin 2 in rat seminiferous tubules during the spermatogenic cycle. *Acta. Med. Okayama*, **56**: 205–209.

Kamitani, A., Yamada, H., Kinuta, M., Watanabe, M., Li, S.A., Matsukawa, T., McNiven, M., Kumon, H., and Takei, K. 2002. Distribution of dynamins in testis and their possible relation to spermatogenesis. *Biochem. Biophys. Res. Commun.*, **294**: 261–267.

Leblond, C.P. and Clermont, Y. 1952. Definition of the stages of the cycle of the seminiferous epithelium in the rat. *Ann. N Y Acad. Sci*., **55**: 548–573.

Lee, E. and De Camilli, P. 2002. Dynamin at actin tails. *Proc. Natl. Acad. Sci. USA*, **99**: 161–166.

Lee, E., Marcucci, M., Daniell, L., Pypaert, M., Weisz, O.A., Ochoa, G.C., Farsad, K., Wenk, M.R., and De Camilli P. 2002. Amphiphysin 2 (Bin1) and T-tubule biogenesis in muscle. *Science*, **297**: 1193–1196.

Lee, N.P. and Cheng, C.Y. 2004a. Ectoplasmic specialization, a testis-specific cell-cell actin-based adherens junction type: is this a potential target for male contraceptive development? *Hum. Reprod. Update*, **10**: 349–369.

Lee, N.P. and Cheng, C.Y. 2004b. Adaptors, junction dynamics, and spermatogenesis. *Biol. Reprod*., **71**: 392–404.

McNiven, M.A., Kim, L., Krueger, E.W., Orth, J.D., Cao, H., and Wong, T.W. 2000. Regulated interactions between dynamin and the actin-binding protein cortactin modulate cell shape. *J. Cell Biol.*, **151**: 187–198.

Mulholland, D.J., Dedhar, S., and Vogl, A.W. 2001. Rat seminiferous epithelium contains a unique junction (ectoplasmic specialization) with signaling properties both of cell/cell and cell/matrix junctions. *Biol. Reprod*., **64**: 396–407.

Mundigl, O., Ochoa, G.C., David, C., Slepnev, V.I., Kabanov, A., and De Camilli, P. 1998. Amphiphysin I antisense oligonucleotides inhibit

neurite outgrowth in cultured hippocampal neurons. *J. Neurosci*., **18**: 93–103.

Mruk, D.D. and Cheng, C.Y. 2004. Cell-cell interactions at the ectoplasmic specialization in the testis. *Trends Endocrinol. Metab*., **15**: 439–447.

Nakata, T., Takemura, R., and Hirokawa, N. 1993. A novel member of the dynamin family of GTP-binding proteins is expressed specifically in the testis. *J. Cell Sci*., **105**: 1–5.

Oakberg, E.F. 1956a. A description of spermiogenesis in the mouse and its use in analysis of the cycle of the seminiferous epithelium and germ cell renewal. *Am. J. Anat*., **99**: 391–413.

Oakberg, E.F. 1956b. Duration of spermatogenesis in the mouse and timing of stages of the cycle of the seminiferous epithelium. *Am. J. Anat.*, **99**: 507–516.

Ochoa, G.C., Slepnev, V.I., Neff, L., Ringstad, N., Takei, K., Daniell, L., Kim, W., Cao, H., McNiven, M., Baron, R., and De Camilli, P. 2000. A functional link between dynamin and the actin cytoskeleton at podosomes. *J. Cell Biol*., **150**: 377–389.

Orth, J.D. and McNiven M.A. 2003. Dynamin at the actin-membrane interface. *Curr. Opin. Cell Biol*., **15**: 31–39.

Peter, B.J., Kent, H.M., Mills, I.G., Vallis, Y., Butler, P.J., Evans, P.R., and McMahon, H.T. 2004. BAR domains as sensors of membrane curvature: the amphiphysin BAR structure. *Science*, **303**: 495–499.

Russell, L. and Clermont, Y. 1976. Anchoring device between Sertoli cells and late spermatids in rat seminiferous tubules. *Anat. Rec*., **185**: 259–278.

Russell, L. 1977. Observations on rat Sertoli ectoplasmic ('junctional') specializations in their association with germ cells of the rat testis. *Tissue Cell*, **9**: 475–498.

Russell, L.D. 1979a. Observations on the inter-relationships of Sertoli cells at the level of the blood- testis barrier: evidence for formation and resorption of Sertoli-Sertoli tubulobulbar complexes during the spermatogenic cycle of the rat. *Am. J. Anat*., **155**: 259–279.

Russell, L.D. 1979b. Further observations on tubulobulbar complexes formed by late spermatids and Sertoli cells in the rat testis. *Anat. Rec*., **194**: 213–232.

Russell, L.D. 1979c. Spermatid-Sertoli tubulobulbar complexes as devices for elimination of cytoplasm from the head region late spermatids of the rat. *Anat. Rec*., **194**: 233–246.

Russell, L.D. and Malone, J.P. 1980. A study of Sertoli-spermatid tubulobulbar complexes in selected mammals. *Tissue Cell*, **12**: 263–285.

Russell, L.D., Goh, J.C., Rashed, R.M., and Vogl, A.W. 1988. The consequences of actin disruption at Sertoli ectoplasmic specialization sites facing spermatids after in vivo exposure of rat testis to cytochalasin D. *Biol. Reprod*., **39**: 105–118.

Schafer, D.A. 2004. Regulating actin dynamics at membranes: a focus on dynamin. *Traffic*, **25**: 463–469.

Takei, K., Haucke, V., Slepnev, V., Farsad, K., Salazar, M., Chen, H., and De Camilli, P. 1998. Generation of coated intermediates of clathrin-mediated endocytosis on protein-free liposomes. *Cell*, **94**: 131–141.

Takei, K., Slepnev, V.I., Haucke, V., and De Camilli, P. 1999. Functional partnership between amphiphysin and dynamin in clathrin-mediated endocytosis. *Nat. Cell Biol*., **1**: 33–39.

Tanii, I., Yoshinaga, K., and Toshimori, K. 1999. Morphogenesis of the acrosome during the final steps of rat spermiogenesis with special reference to tubulobulbar complexes. *Anat. Rec.*, **256**: 195–201.

Vaid, K.S., Guttman, J.A., Babyak, N., Deng, W., McNiven, M.A, Mochizuki, N., Finlay, B.B., and Vogl, A.W. 2007. The role of dynamin 3 in the testis. *J. Cell Physiol*., **210**: 644–654.

Watanabe, M., Tsutsui, K., Hosoya, O., Tsutsui, K., Kumon, H., and Tokunaga, A. 2001. Expression of amphiphysin I in Sertoli cells and its implication in spermatogenesis. *Biochem. Biophys. Res. Commun*., **287**: 739–745.

Witke, W., Podtelejnikov, A.V., Di Nardo, A., Sutherland, J.D., Gurniak, C.B., Dotti, C., and Mann, M. 1998. In mouse brain profilin I and profilin II associate with regulators of the endocytic pathway and actin assembly. *EMBO J.*, **17**: 967–976.

Yoshida, Y., Kinuta, M., Abe, T., Liang, S., Araki, K., Cremona, O., Di Paolo, G., Moriyama, Y., Yasuda, T., De Camilli, P., and Takei, K. 2004. The stimulatory action of amphiphysin on dynamin function is dependent on lipid bilayer curvature. *EMBO J*., **23**: 3483–3491.

*(Received for publication, July 17, 2007 and accepted, August 2, 2007)*